Impact of radiation from primordial black holes on the 21-cm angular-power spectrum in the dark ages

Yupeng Yang

School of Physics and Physical Engineering, Qufu Normal University, Qufu, Shandong 273165, China

(Received 17 May 2022; accepted 30 November 2022; published 15 December 2022)

We investigate the impact of radiation from primordial black holes (PBHs), in the mass range of $10^{15} \lesssim M_{\rm PBH} \lesssim 10^{17}$ g and $10^2 \lesssim M_{\rm PBH} \lesssim 10^4 M_\odot$, on the 21-cm angular-power spectrum in the dark ages. PBHs in the former mass range affect the 21-cm angular-power spectrum through the evaporation known as Hawking radiation, while the radiation from the accretion process in the latter mass range. In the dark ages, radiation from PBHs can increase the ionization fraction and temperature of the intergalactic medium, change the global 21-cm differential brightness temperature and then affect the 21-cm angular-power spectrum. Taking into account the effects of PBHs, we find that in the dark ages, $30 \lesssim z \lesssim 100$, the amplitude of the 21-cm angular-power spectrum is decreased depending on the mass and mass fraction of PBHs. We also investigate the potential constraints on the mass fraction of PBHs in the form of dark matter for the future radio telescope in lunar orbit or on the far side surface of the Moon.

DOI: 10.1103/PhysRevD.106.123508

I. INTRODUCTION

In the standard cosmological model, dark matter makes up about 27% of the Universe [1]. Although many astronomical observations have confirmed the existence of dark matter, its nature has so far been unknown. Among the many dark matter models, weakly interacting massive particles (WIMPs) is the most important one [2,3]. However, so far, all relevant experiments to detect WIMPs have not found any signs of them. Other dark matter models, such as primordial black holes (PBHs), have attracted extensive attention again [4–18]. Recently, the gravitational waves generated by the merger of black holes detected by LIGO/Virgo may be partly caused by PBHs [19–25].

PBHs can be formed by the collapse of large density perturbation existing in the early Universe and their masses spread a wide range (see, e.g., Refs. [5,26,27]). A PBH smaller than $M_{\rm PBH} \sim 10^{17}$ g loses mass through evaporation due to Hawking radiation [5,28–34]. A massive PBH with mass $M_{\rm PBH} \gtrsim 10^2 M_\odot$ radiates energy in the process of accretion [35–41]. The extra energy injection from PBHs can affect the evolution of the intergalactic medium (IGM). The changes in the thermal history of the IGM will be reflected in, e.g., the anisotropy of the cosmic microwave background (CMB) and the global 21-cm signal [42–53].

Recently, the experiment to detect the global epoch of reionization signature reported the detection of the global 21-cm signal centered at redshift $z \sim 17$ with an amplitude twice as large as expected [54]. Although this result needs to be further verified by other experiments, the observation can be used to study the related properties of PBHs, such as limiting their mass fraction. According to the theory, there are also 21-cm absorption signals in the dark ages of the Universe ($30 \lesssim z \lesssim 100$) [55,56], and these radio signals have been redshifted to the low frequency range ($14 \lesssim \nu_{21} \lesssim 46$ MHz). The Earth's ionosphere makes it impossible to detect these low-frequency signals from the Earth. Radio telescopes in orbit around the moon or on the far side of the moon have been proposed to avoid the influence of the ionosphere [57–63]. In Ref. [39], the authors have investigated the effect of PBH accretion radiation on the global 21-cm signal in the dark ages, and explored the ability of future radio telescopes to limit the mass fraction of PBHs for the mass range of $10 \lesssim M_{\rm PBH} \lesssim 10^4 M_\odot$. Although the resulting constraints are not the strongest, they are still competitive with that of the lower redshift period because the dark ages are less affected by the formation of cosmic structures. Similar to the anisotropy of the cosmic microwave background, the 21-cm signals can also be studied using the angular-power spectrum [64–67]. The influence of dark matter annihilation on the 21-cm angular-power spectrum in the cosmic dawn has been studied in, e.g., Ref. [68].

In this paper, we focus on the influence of PBHs on the 21-cm angular-power spectrum in the dark ages. We mainly investigate the radiation from the evaporation and accretion process of PBHs, corresponding to the mass range of

$10^{15} \lesssim M_{\rm PBH} \lesssim 10^{17}$ g and $10^2 \lesssim M_{\rm PBH} \lesssim 10^4 M_\odot$, respectively.[1] In view of a future extraterrestrial radio telescope, we investigate the ability of future detection of the 21-cm angular-power spectrum to limit the abundance of PBHs.

This paper is organized as follows. In Sec. II we investigate the influence of PBHs on the thermal history of the IGM and the global 21-cm signal in the dark ages. The 21-cm angular-power spectrum including PBHs and the future potential upper limits on the abundance of PBHs are discussed in Sec. III. The conclusions are given in Sec. IV. Throughout the paper we will use the cosmological parameters from Planck-2018 results [1].

II. THE GLOBAL 21-CM SIGNAL IN THE DARK AGES INCLUDING PBHs

A. The thermal history of the IGM including PBHs

The changes in the thermal history of the Universe due to the injection of extra energy have been investigated by previous works (see, e.g., Refs. [69–71]). Here we review the main points and one can refer to, e.g., Refs. [69,71] for more details.

The interactions between the particles emitted from PBHs with those existing in the Universe result in the changes of the thermal history of the IGM. Taking into account the effects of heating, ionization, and excitation, the changes of the degree of ionization (x_e) and the temperature of IGM (T_k) with the redshift are governed by the following equations [69,72]:

$$(1+z)\frac{dx_e}{dz} = \frac{1}{H(z)}[R_s(z) - I_s(z) - I_{\rm PBH}(z)], \quad (1)$$

$$(1+z)\frac{dT_k}{dz} = \frac{8\sigma_T a_R T_{\rm CMB}^4}{3m_e c H(z)}\frac{x_e(T_k - T_{\rm CMB})}{1+f_{\rm He}+x_e} - \frac{2}{3k_B H(z)}\frac{K_{\rm PBH}}{1+f_{\rm He}+x_e} + 2T_k, \quad (2)$$

where $R_s(z)$ and $I_s(z)$ are the recombination and ionization rate for the case with no PBHs, respectively. The ionization and heating rate caused by PBHs can be written as follows [44,73–75]:

$$I_{\rm PBH} = f_i(z)\frac{1}{n_b}\frac{1}{E_0}\frac{{\rm d}E}{{\rm d}V{\rm d}t}\bigg|_{\rm PBH} \quad (3)$$

$$K_{\rm PBH} = f_h(z)\frac{1}{n_b}\frac{{\rm d}E}{{\rm d}V{\rm d}t}\bigg|_{\rm PBH}, \quad (4)$$

where n_b is the number density of baryon. E_0 stands for the ground state energy of the hydrogen atom. $f(z)$ corresponds to the energy fraction injected into the IGM for ionization, heating and exciting, respectively. It has been studied in detail, e.g., Refs. [37,71,76], and we use the public code EXOCLASS [77,78] to calculate $f(z)$ numerically.

For evaporating PBHs, the energy injection rate per unit volume is given by [74,79]

$$\frac{{\rm d}E}{{\rm d}V{\rm d}t}\bigg|_{\rm PBH,eva} = f_{\rm pbh}\frac{\rho_{\rm DM}}{M_{\rm PBH}}\frac{{\rm d}M_{\rm PBH}}{{\rm d}t}, \quad (5)$$

where $f_{\rm pbh} = \rho_{\rm PBH}/\rho_{\rm DM}$. Here we have adopted a monochromatic PBH mass function for our calculations. The mass-loss rate of a black hole is [5,28]

$$\frac{dM_{\rm BH}}{{\rm d}t} = -5.34\times 10^{25} f(M_{\rm BH})\left(\frac{M_{\rm BH}}{\rm g}\right)^{-2}\ {\rm g\,s^{-1}}, \quad (6)$$

where $f(M_{\rm BH})$ is the number of particle species emitted directly and we have used the formula given in Ref. [29].

For accreting PBHs, the energy injection rate per unit volume can be written as [37,38]

$$\frac{{\rm d}E}{{\rm d}V{\rm d}t}\bigg|_{\rm PBH,acc} = f_{\rm pbh}\frac{\rho_{\rm DM}}{M_{\rm PBH}}L_{\rm acc,PBH}, \quad (7)$$

where $L_{\rm acc,PBH}$ is the accretion luminosity, which is proportional to the Bondi-Hoyle rate $\dot{M}_{\rm HB}$ [37]:

$$L_{\rm acc,PBH} = \epsilon \dot{M}_{\rm HB} c^2, \quad (8)$$

where ϵ is the radiative efficiency depending on the accretion details. The authors of [38] made a detailed analysis of the accretion process of PBHs, finding $\epsilon = 10^{-5}(10^{-3})\dot{m}$ for collisional ionization (photoionization). Here we use $\epsilon = 10^{-5}\dot{m}$ for our calculations, corresponding to the conservative case. $\dot{m}$ is the dimensionless Bondi-Hoyle accretion rate, which is in the form of the Eddington luminosity $L_{\rm Edd}$ as $\dot{m} = \dot{M}_{\rm HB}c^2/L_{\rm Edd}$.

In order to get the thermal history of the IGM for the case with PBHs, we have modified the public code RECFAST in CAMB[2] to solve the differential equations (1) and (2) numerically [69,70,73–75,79]. The changes of T_k with redshift are shown in Fig. 1. In general, the injection of extra energy from PBHs raises the temperature of the IGM, and these effects are more pronounced at lower redshifts.

B. The global 21-cm signal including PBHs

Here we review the main issues about the global 21-cm signal. For more details and in-depth discussion, one can refer to, e.g., Refs. [55,56] and references therein.

[1] A PBH with mass $M_{\rm PBH} \lesssim 10^{15}$ g has a shorter lifetime than the age of the Universe [5]. Here we only consider a PBH with mass greater than 10^{15} g. It should be pointed out that the lower mass PBH can still affect the 21-cm angular-power spectrum in the dark ages.

[2] https://camb.info/.

The global 21-cm signal is usually described by the differential brightness temperature δT_{21}. Relative to the CMB background, δT_{21} can be written as follows [80–82]:

$$\delta T_{21} = 26(1-x_e)\left(\frac{\Omega_b h}{0.02}\right)\left[\frac{1+z}{10}\frac{0.3}{\Omega_m}\right]^{\frac{1}{2}} \times \left(1-\frac{T_{\rm CMB}}{T_s}\right)\ {\rm mK}, \tag{9}$$

where Ω_b and Ω_m are the density parameters of baryonic matter and dark matter, respectively. h is the reduced Hubble constant. T_s is the spin temperature defined as [55,56]

$$\frac{n_1}{n_0} = 3\ \exp\left(-\frac{0.068K}{T_s}\right), \tag{10}$$

where n_0 and n_1 are the number densities of hydrogen atoms in triplet and singlet states, respectively. Specifically, the spin temperature can be written in the form of a weighted mean of the CMB temperature ($T_{\rm CMB}$) and the IGM temperature (T_k) [80,83]

$$T_s = \frac{T_{\rm CMB} + (y_\alpha + y_c)T_k}{1 + y_\alpha + y_c}, \tag{11}$$

where y_α corresponds to the Wouthuysen-Field effect and we use the formula given in, e.g., Refs. [73,83,84]:

$$y_\alpha = \frac{P_{10}}{A_{10}}\frac{0.068}{T_k}\,{\rm e}^{-\frac{0.3\sqrt{1+z}}{T_k^{2/3}}}\left(1+\frac{0.4}{T_k}\right)^{-1}, \tag{12}$$

where $A_{10} = 2.85\times10^{-15}\ {\rm s}^{-1}$ is the Einstein coefficient of hyperfine spontaneous transition. P_{10} is the radiative deexcitation rate due to Lyα photons [55,56]. Taking into account the collisions between hydrogen atoms and other particles, y_c can be written as [82–86]

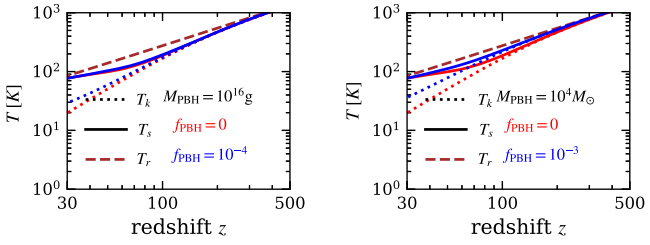

FIG. 1. The changes of the IGM temperature (T_k, dotted lines) and the spin temperature (T_s, solid lines) with redshift. Left: evaporating PBH with mass $M_{\rm PBH} = 10^{16}$ g and mass fraction $f_{\rm PBH} = 10^{-4}$. Right: accreting PBH with mass $M_{\rm PBH} = 10^4 M_\odot$ and mass fraction $f_{\rm PBH} = 10^{-3}$. For comparison, we also show the plots for the case with no PBH $f_{\rm PBH} = 0$ (red lines). The CMB temperature (T_r) is also shown (brown dashed line).

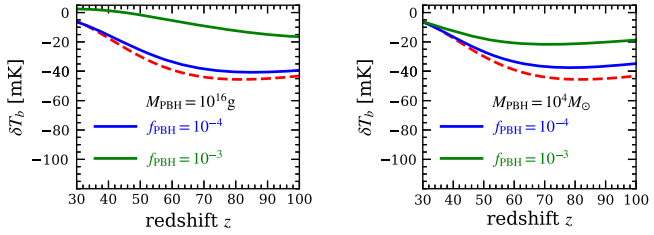

FIG. 2. The changes of the differential brightness temperature δT_{21} with redshift for mass fraction $f_{\rm PBH} = 10^{-4}$ (blue solid line) and $f_{\rm PBH} = 10^{-3}$ (green solid line). Left: evaporating PBH with mass $M_{\rm PBH} = 10^{16}$ g. Right: accreting PBH with mass $M_{\rm PBH} = 10^4 M_\odot$. The case with no PBH $f_{\rm PBH} = 0$ is also shown (red dashed line).

$$y_c = \frac{0.068(C_{\rm HH} + C_{\rm eH} + C_{\rm pH})}{A_{10}T_k}, \tag{13}$$

where $C_{\rm HH,eH,pH}$ are the deexcitation rates of collisions [82,84–86].

The changes of the spin temperature T_s with redshift are shown in Fig. 1. It can be seen that T_s becomes larger than that with no PBH, depending on the mass and mass fraction of PBH. The changes of the differential brightness temperature δT_{21} with redshift are shown in Fig. 2. The amplitude of the 21-cm absorption signal is decreased due to the influence of PBH. For a larger mass fraction of PBH with a fixed mass, the emission signal appears as shown in Fig. 2 for $f_{\rm PBH} = 10^{-3}$ with $M_{\rm PBH} = 10^{16}$ g.

III. THE 21-CM ANGULAR-POWER SPECTRUM AND UPPER LIMITS ON THE MASS FRACTION OF PBHs

Similar to the CMB anisotropy, the fluctuations of δT_{21} can also be described by the 21-cm angular-power spectrum, which can be calculated by using a standard Boltzmann code. The calculation details of 21-cm angular-power spectrum can be found in Ref. [64] and the numerical code is available in CAMB. Here we have used the public code CAMB for our calculations, which has been used in the previous section to investigate the thermal history of the IGM including the effects of PBHs. The 21-cm angular-power spectrum at redshift $z = 50$ is shown in Fig. 3.

For the case with no PBH, the amplitude of the 21-cm angular-power spectrum is about 1–3 mK for $l \sim 10^3$–10^5. Since the angular-power spectrum is roughly proportional to $|\delta T_{21}|$ [56,64], therefore, for the case with PBH, the angular-power spectrum is decreased depending on the mass and mass fraction of PBH. In Fig. 4, we also show the 21-cm angular-power spectrum for a scale $l = 1400$ in the redshift range $30 \lesssim z \lesssim 100$. For the case with no PBH, the largest amplitude of the angular-power spectrum appears at redshift

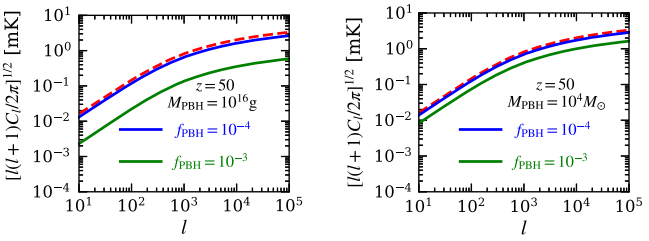

FIG. 3. The 21-cm angular-power spectrum at redshift $z = 50$ including PBH for mass fraction $f_{\rm PBH} = 10^{-4}$ (blue solid line) and $f_{\rm PBH} = 10^{-3}$ (green solid line). Left: evaporating PBH with mass $M_{\rm PBH} = 10^{16}$ g. Right: accreting PBH with mass $M_{\rm PBH} = 10^4 M_\odot$.

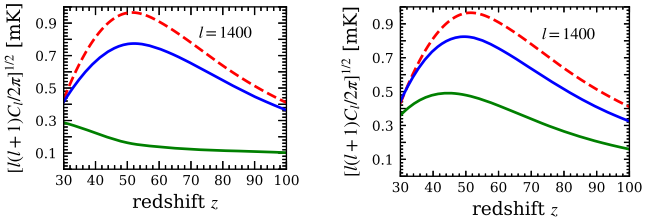

FIG. 4. The evolution of the 21-cm angular-power spectrum with redshift in the dark ages ($30 \lesssim z \lesssim 100$) for a scale $l = 1400$. The line style is the same as in Figs. 2 and 3. Left: evaporating PBH with mass $M_{\rm PBH} = 10^{16}$ g. Right: accreting PBH with mass $M_{\rm PBH} = 10^4 M_\odot$.

$z \sim 50$.[3] Including the effects of PBH, the largest amplitude shifts to the lower redshifts.

The 21-cm signal ($\nu_{21} = 1421$ MHz) from the redshift range $30 \lesssim z \lesssim 100$ has been redshifted into the frequency range $14 \lesssim \nu_{21} \lesssim 46$ MHz. Due to the influence of the Earth's ionosphere, it is difficult to detect these low frequency signals from the Earth. A radio telescope, either in lunar orbit or on the far side surface of the Moon, has been proposed to detect these radio signals [57–62]. For a radio telescope, the uncertainty of the C_l at a multipole l is [67,88,89]

$$\sigma_{C_l} = \sqrt{\frac{2(C_l + C_l^N)^2}{f_{\rm sky}(2l+1)}}, \tag{14}$$

where C_l^N is the noise power spectrum [67,88]

$$l^2 C_l^N = \frac{(2\pi)^2 T_{\rm sky}^2}{\Delta\nu t_{\rm obs} f_{\rm cover}^2}\left(\frac{l}{l_{\rm max}}\right)^2, \tag{15}$$

where $t_{\rm obs}$ is the observation time, $l_{\rm max}$ is the maximum multipole observable, and $f_{\rm cover}$ is the array covering factor. $T_{\rm sky}$ is the sky temperature. For the low frequency range, $\nu < 100$ MHz, $T_{\rm sky}$ is dominated by the galactic synchrotron radiation background and scales as $\nu^{-\alpha}$ [56,90–95]. A more detailed analysis of $T_{\rm sky}$ can be also found in, e.g., Ref. [96]. Here we adopted the approximated form given in Ref. [92]:

$$T_{\rm sky} = 16.3 \times 10^6 \left(\frac{\nu}{2\ {\rm MHz}}\right)^{-2.53}\ {\rm K}. \tag{16}$$

Another approximated form usually used is $T_{\rm sky} = 180(\nu/180\ {\rm MHz})^{-2.6}$ K; see, e.g., Refs. [56,97]. Note that the differences between two formulas have a negligible impact on the estimation of our final results.

For a future radio telescope, e.g., on the lunar surface [88,98], with an array size $D \sim 300$ km, the maximum multipole could reach $l_{\rm max} \sim 10^5$ at redshift $z \sim 50$. Therefore, for the array covering factor $f_{\rm cover} \sim 0.75$ and bandwidth $\Delta\nu \sim 50$ MHz, the uncertainty of the C_l at $z = 50$ for $l = 1400$ could be $\sigma_{C_l} \sim 0.02$ mK for 1000 hours observation time and $f_{\rm sky} \sim 1$. Therefore, a large deviation of the 21-cm angular-power spectrum from the default case could be detected for the future radio telescope. On the other hand, future observations of the 21-cm angular-power spectrum can be used to put limits on the abundance of PBHs. Here we will make a simple study of the abundance of PBHs for the future detection, and more detailed studies are left for future work.

Instead of focusing on the sensitivity of a specific radio telescope, we have set $\sigma_{C_l} = 0.1$ and 0.01 mK for our calculations, which could be achieved in the future. Moreover, for simplicity, we have focused on the maximum sensitivity at a specific scale l instead of all scales [67]. By requiring the deviation of the 21-cm angular-power spectrum less than σ_{C_l} for $l = 1400$ at redshift $z = 50$, we find the upper limits on the mass fraction of PBHs $f_{\rm PBH}$, which are shown in Fig. 5. For evaporating PBHs, the strongest limit is $f_{\rm PBH} \sim 10^{-8}(10^{-9})$ for $\sigma_{C_l} = 0.1$ (0.01) mK for $M_{\rm PBH} \sim 10^{15}$ g. For accreting PBHs, the

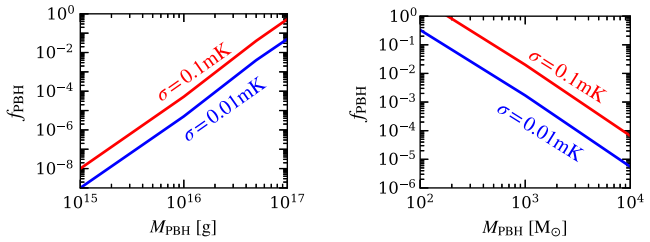

FIG. 5. Upper limits on the mass fraction of PBHs for future radio detection. Instead of focusing on the sensitivity of a specific radio telescope, we have set $\sigma_{C_l} = 0.1$ (red line) and 0.01 mK (blue line) for our calculations. Left: evaporating PBH in the mass range of $10^{15} \lesssim M_{\rm PBH} \lesssim 10^{16}$ g. Right: accreting PBH in the mass range of $10^2 \lesssim M_{\rm PBH} \lesssim 10^4 M_\odot$.

[3]Similar results can also be found for other scales [55,87].

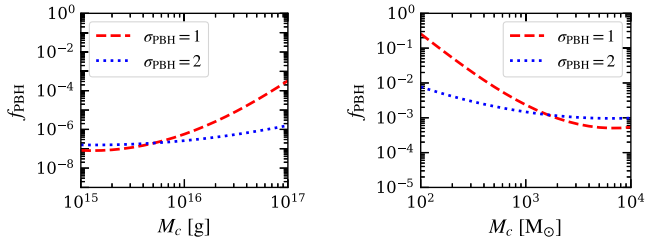

FIG. 6. Upper limits on the mass fraction of PBHs for extended mass function for $\sigma_{\rm PBH}=1$ (dashed line) and 2 (dotted line). Here we have set $\sigma_{C_l}=0.1$ mK. Left: evaporating PBH in the mass range of $10^{15}\lesssim M_{\rm PBH}\lesssim 10^{16}$ g. Right: accreting PBH in the mass range of $10^2\lesssim M_{\rm PBH}\lesssim 10^4 M_\odot$.

strongest limit is $f_{\rm PBH}\sim 6\times 10^{-5}(10^{-6})$ for $\sigma_{C_l}=0.1$ (0.01) mK for $M_{\rm PBH}\sim 10^4 M_\odot$. Note that these constraints are comparable to the existing ones [5]. Since these limits are from the dark ages, where the influence of astrophysical factors is smaller than that in the later period, therefore, future extraterrestrial detection of the radio signal can give very competitive results for limiting the mass fraction of PBHs.

Although the monochromatic PBH mass function has been used usually, the extended mass function should be more realistic as predicted by many formation scenarios; see, e.g., Refs. [99–107]. Here we also investigate the constraints on $f_{\rm PBH}$ for extended PBH mass function. We consider one of the typical extended PBH mass functions, log-normal distribution [105,108], as follows:

$$\Psi(M)=\frac{1}{\sqrt{2\pi}\sigma_{\rm PBH}M}\exp\left[-\frac{(\log {\rm M}-\log {\rm M}_c)^2}{2\sigma_{\rm PBH}^2}\right]. \quad (17)$$

Using the constraints from the monochromatic PBH mass function, one can derive the upper limits on $f_{\rm PBH}$ for extended PBH mass distribution [43,51,105,109],

$$f_{\rm PBH}\leq\left[\int dM\frac{\Psi(M,M_c,\sigma_{\rm PBH})}{f'_{\rm PBH}(M)}\right]^{-1}, \quad (18)$$

where $f'_{\rm PBH}(M)$ is the constraint for monochromatic PBH mass function shown in Fig. 5. The upper limits on $f_{\rm PBH}$ for extended PBH mass function are shown in Fig. 6.[4]

Another important issue for the influence of PBHs on the 21-cm angular-power spectrum is the Poissonian fluctuation in the number density of PBHs, which has an extra contribution to the standard matter power spectrum [88,110–113]. Compared with the effects of PBHs considered here, the amplitude of the 21-cm angular-power spectrum is increased due to Poissonian fluctuation. As shown in, e.g., Refs. [88,112], Poissonian fluctuation has a large effect at lower redshifts ($z\lesssim 50$) or on smaller scales ($l\gtrsim 10^3$), depending on the related parameters. At higher redshifts, the Poissonian contribution becomes smaller even on smaller scales [88,112]. Given the opposite effects of the radiation and Poissonian fluctuation of PBHs on the 21-cm angular-power spectrum, it is expected that the future detection of power spectrum at higher redshifts can significantly reduce the impact of Poissonian contribution.

Many other factors can also affect the 21-cm angular-power spectrum [64]. Correspondingly, the detection of the 21-cm angular-power spectrum can be used to investigate those factors, such as the primordial power spectrum [$\mathcal{P}_\mathcal{R}(k)$], which is related to the formation scenario of PBHs. The primordial power spectrum at large scales (small k) has been constrained by many observations, which is basically consistent with the scale invariant spectrum predicted by the popular inflation model [114–116]. In general, the primordial power spectrum at small scales (large k) should be enhanced in order to form PBHs; see, e.g., Refs. [112,117–134]. Many different formation scenarios of PBHs, corresponding to the different forms of $\mathcal{P}_\mathcal{R}(k)$ and matching the measurements on small scales, have been proposed. As shown in, e.g., Ref. [112], the 21-cm power spectrum (three dimensions) can be used to investigate these different scenarios since the 21-cm signal covers smaller scales and many more modes than those such as CMB measurements. In theory, the 21-cm angular-power spectrum can also be used to study different formation scenarios of PBHs. Compared with the scale invariant spectrum, the enhancement of $\mathcal{P}_\mathcal{R}(k)$ at small scale (larger k) can result in the increasing of the 21-cm angular-power spectrum at small scale (large l) [112]. It is expected that these deviations from the standard power spectrum, corresponding to the different formation scenarios of PBHs, would also be examined by future detection of the 21-cm angular-power spectrum. We will conduct a detailed analysis of the relevant issues in future work.

Note that in obtaining the above limits, we have fixed other cosmological parameters except $f_{\rm PBH}$. On the other hand, the parameter $f_{\rm PBH}$ can affect the estimation of cosmological parameters [65], and the details of these effects are complicated to analyze. Roughly, for example, the 21-cm angular-power spectrum is proportional to $|\delta T_{21}|$ [56,64], which is related to Ω_b as shown in Eq. (9). Decreasing (increasing) the baryon density will result in lowering (boosting) the amplitude of 21-cm angular-power spectrum. Therefore, it is expected that Ω_b and $f_{\rm PBH}$ should be positively correlated in view of the 21-cm angular-power spectrum in the dark ages. Note that the analysis here is simple. A complete multiparameter analysis should be carried out by the statistical method such as Markov chain Monte Carlo, and we will perform these analyses in future work.

[4]Note that the extended mass function should be also included in the calculations of the energy injection into IGM [51,107]. The final constraints should be different by several factors [51,74].

IV. CONCLUSIONS

We have investigated the impact of PBHs on the thermal history of IGM and the 21-cm angular-power spectrum in the dark ages. Previous works mainly focused on the effects of the radiation from accreting PBHs on the global 21-cm signal and 21-cm power spectrum in the cosmic dawn and epoch of reionization. Here we have also focused on the evaporating PBHs in the mass range of $10^{15} \lesssim M_{\rm PBH} \lesssim 10^{16}$ g, besides the accreting PBHs in the mass range of $10^2 \lesssim M_{\rm PBH} \lesssim 10^4 M_\odot$. The radiation from PBHs results in increasing the gas and spin temperature compared with the case with no PBHs. The amplitude of the 21-cm absorption signal is decreased, and the emission signal appears for a larger mass fraction of PBHs. The fluctuations of the 21-cm differential brightness temperature can be described by the 21-cm angular-power spectrum. Taking into account the effects of PBHs, the 21-cm angular-power spectrum is decreased in the dark ages depending on the mass and mass fraction of PBHs. The peak value of the 21-cm angular-power spectrum appears at redshift $z \sim 50$ for the case with no PBHs, and shifts to the lower redshifts including PBHs.

The 21-cm signals from the dark ages have been redshifted into the lower frequency $14 \lesssim \nu_{21} \lesssim 46$ MHz ($30 \lesssim z \lesssim 100$). It is difficult to detect these radio signals from the Earth due to the influence of Earth's ionosphere. Extraterrestrial radio telescopes, such as in lunar orbit or on the lunar surface, have been proposed. In view of the future radio telescopes, we have estimated the upper limits on the mass fraction of PBHs. Instead of focusing on a specific radio telescope, we have set the uncertainty $\sigma_{C_l} = 0.1$ and 0.01 mK, which can be achieved in the future, for our calculations. For a evaporating PBH with mass $M_{\rm PBH} \sim 10^{15}$ g, the upper limit is $f_{\rm PBH} \sim 10^{-8}(10^{-9})$ for $\sigma_{\rm Cl} = 0.1(0.01)$ mK. For a accreting PBH with mass $M_{\rm PBH} \sim 10^4 M_\odot$, the upper limit is $f_{\rm PBH} \sim 6 \times 10^{-5}(10^{-6})$ for $\sigma_{\rm Cl} = 0.1(0.01)$ mK. Compared with the cosmic dawn and epoch of reionization, the dark ages is less affected by the astrophyscial factors. Therefore, the detection of the 21-cm signal or angular-power spectrum in the dark ages will be of great significance to reveal the relevant properties of PBHs.

ACKNOWLEDGMENTS

Y. Y. thanks Dr. Bin Yue, Yan Gong and Yidong Xu for the helpful discussions and suggestions. This work is supported by the Shandong Provincial Natural Science Foundation (Grant No. ZR2021MA021). Y. Y. is supported in part by the Youth Innovations and Talents Project of Shandong Provincial Colleges and Universities (Grant No. 201909118) and the Taishan Scholar Project of Shandong Province (Grant No. tsqn202103062).

[1] N. Aghanim *et al.* (Planck Collaboration), Astron. Astrophys. **641**, A6 (2020); **652**, C4(E) (2021).
[2] G. Bertone, D. Hooper, and J. Silk, Phys. Rep. **405**, 279 (2005).
[3] G. Jungman, M. Kamionkowski, and K. Griest, Phys. Rep. **267**, 195 (1996).
[4] Z.-C. Zou and Y.-F. Huang, Astrophys. J. Lett. **928**, L13 (2022).
[5] B. J. Carr, K. Kohri, Y. Sendouda, and J. Yokoyama, Phys. Rev. D **81**, 104019 (2010).
[6] S. Bird *et al.*, arXiv:2203.08967.
[7] B. Carr and F. Kuhnel, Sci. Post Phys. Lect. Notes **48**, 1 (2022).
[8] Y.-P. Wu, E. Pinetti, and J. Silk, Phys. Rev. Lett. **128**, 031102 (2022).
[9] M. M. Flores and A. Kusenko, arXiv:2108.08416.
[10] F. Zhang, J. Lin, and Y. Lu, Phys. Rev. D **104**, 063515 (2021); **104**, 129902(E) (2021).
[11] P. Villanueva-Domingo, O. Mena, and S. Palomares-Ruiz, Front. Astron. Space Sci. **8**, 87 (2021).
[12] G. Hasinger, J. Cosmol. Astropart. Phys. 07 (2020) 022.
[13] X.-F. Zhang, J.-G. Cheng, B.-Y. Zhu, T.-C. Liu, Y.-F. Liang, and E.-W. Liang, Phys. Rev. D **105**, 043011 (2022).
[14] K. M. Belotsky, A. D. Dmitriev, E. A. Esipova, V. A. Gani, A. V. Grobov, M. Y. Khlopov, A. A. Kirillov, S. G. Rubin, and I. V. Svadkovsky, Mod. Phys. Lett. A **29**, 1440005 (2014).
[15] R. Laha, Phys. Rev. Lett. **123**, 251101 (2019).
[16] B. Dasgupta, R. Laha, and A. Ray, Phys. Rev. Lett. **125**, 101101 (2020).
[17] R. Laha, J. B. Muñoz, and T. R. Slatyer, Phys. Rev. D **101**, 123514 (2020).
[18] R. Laha, P. Lu, and V. Takhistov, Phys. Lett. B **820**, 136459 (2021).
[19] S. Bird, I. Cholis, J. B. Muñoz, Y. Ali-Haïmoud, M. Kamionkowski, E. D. Kovetz, A. Raccanelli, and A. G. Riess, Phys. Rev. Lett. **116**, 201301 (2016).
[20] S. Clesse and J. Garcia-Bellido, Phys. Dark Universe **38**, 101111 (2022).
[21] H. Deng, J. Cosmol. Astropart. Phys. 04 (2021) 058.
[22] G. Franciolini, V. Baibhav, V. De Luca, K. K. Y. Ng, K. W. K. Wong, E. Berti, P. Pani, A. Riotto, and S. Vitale, Phys. Rev. D **105**, 083526 (2022).
[23] Z.-C. Chen, C. Yuan, and Q.-G. Huang, Phys. Lett. B **829**, 137040 (2022).
[24] G. Hütsi, M. Raidal, V. Vaskonen, and H. Veermäe, J. Cosmol. Astropart. Phys. 03 (2021) 068.

[25] A. Ashoorioon, K. Rezazadeh, and A. Rostami, Phys. Lett. B **835**, 137542 (2022).
[26] B. J. Carr, in 59th Yamada Conference on Inflating Horizon of Particle Astrophysics and Cosmology, 2005, arXiv:astro-ph/0511743.
[27] M. Y. Khlopov, Res. Astron. Astrophys. **10**, 495 (2010).
[28] A. S. Josan, A. M. Green, and K. A. Malik, Phys. Rev. D **79**, 103520 (2009).
[29] H. Tashiro and N. Sugiyama, Phys. Rev. D **78**, 023004 (2008).
[30] D. N. Page, Phys. Rev. D **13**, 198 (1976).
[31] D. N. Page, Phys. Rev. D **14**, 3260 (1976).
[32] D. N. Page, Phys. Rev. D **16**, 2402 (1977).
[33] K. Kohri, T. Nakama, and T. Suyama, Phys. Rev. D **90**, 083514 (2014).
[34] A. Ray, R. Laha, J. B. Muñoz, and R. Caputo, Phys. Rev. D **104**, 023516 (2021).
[35] M. Ricotti, Astrophys. J. **662**, 53 (2007).
[36] M. Ricotti, J. P. Ostriker, and K. J. Mack, Astrophys. J. **680**, 829 (2008).
[37] V. Poulin, P. D. Serpico, F. Calore, S. Clesse, and K. Kohri, Phys. Rev. D **96**, 083524 (2017).
[38] Y. Ali-Haïmoud and M. Kamionkowski, Phys. Rev. D **95**, 043534 (2017).
[39] Y. Yang, Mon. Not. R. Astron. Soc. **508**, 5709 (2021).
[40] B. Carr, F. Kuhnel, and L. Visinelli, Mon. Not. R. Astron. Soc. **501**, 2029 (2021).
[41] R. D'Agostino, R. Giambò, and O. Luongo, arXiv:2204.02098.
[42] U. Mukhopadhyay, D. Majumdar, and A. Halder, J. Cosmol. Astropart. Phys. 10 (2022) 099.
[43] J. Cang, Y. Gao, and Y.-Z. Ma, J. Cosmol. Astropart. Phys. 03 (2022) 012.
[44] Y. Yang, Phys. Rev. D **104**, 063528 (2021).
[45] P. K. Natwariya, A. C. Nayak, and T. Srivastava, Mon. Not. R. Astron. Soc. **510**, 4236 (2022).
[46] S. Mittal, A. Ray, G. Kulkarni, and B. Dasgupta, J. Cosmol. Astropart. Phys. 03 (2022) 030.
[47] H. Tashiro and K. Kadota, Phys. Rev. D **103**, 123532 (2021).
[48] Y. Yang, Eur. Phys. J. Plus **135**, 690 (2020).
[49] L. Chen, Q.-G. Huang, and K. Wang, J. Cosmol. Astropart. Phys. 12 (2016) 044.
[50] K. J. Mack and D. H. Wesley, arXiv:0805.1531.
[51] J. Cang, Y. Gao, and Y. Ma, J. Cosmol. Astropart. Phys. 05 (2021) 051.
[52] O. Mena, S. Palomares-Ruiz, P. Villanueva-Domingo, and S. J. Witte, Phys. Rev. D **100**, 043540 (2019).
[53] A. K. Saha and R. Laha, Phys. Rev. D **105**, 103026 (2022).
[54] J. D. Bowman, A. E. E. Rogers, R. A. Monsalve, T. J. Mozdzen, and N. Mahesh, Nature (London) **555**, 67 (2018).
[55] J. R. Pritchard and A. Loeb, Rep. Prog. Phys. **75**, 086901 (2012).
[56] S. Furlanetto, S. P. Oh, and F. Briggs, Phys. Rep. **433**, 181 (2006).
[57] X. Chen *et al.*, arXiv:1907.10853.
[58] J. Burns *et al.*, arXiv:2103.05085.
[59] J. O. Burns, Phil. Trans. R. Soc. A **379**, 20190564 (2021).
[60] J. Burns *et al.*, arXiv:2103.08623.
[61] L. Plice, K. Galal, and J. O. Burns, arXiv:1702.00286.
[62] X. Chen *et al.*, arXiv:1907.10853.
[63] Y. Shi, F. Deng, Y. Xu, F. Wu, Q. Yan, and X. Chen, Astrophys. J. **929**, 32 (2022).
[64] A. Lewis and A. Challinor, Phys. Rev. D **76**, 083005 (2007).
[65] A. Loeb and M. Zaldarriaga, Phys. Rev. Lett. **92**, 211301 (2004).
[66] M. G. Santos, A. Cooray, and L. Knox, Astrophys. J. **625**, 575 (2005).
[67] M. Zaldarriaga, S. R. Furlanetto, and L. Hernquist, Astrophys. J. **608**, 622 (2004).
[68] A. Natarajan and D. J. Schwarz, Phys. Rev. D **80**, 043529 (2009).
[69] X. Chen and M. Kamionkowski, Phys. Rev. D **70**, 043502 (2004).
[70] L. Zhang, X. Chen, M. Kamionkowski, Z.-g. Si, and Z. Zheng, Phys. Rev. D **76**, 061301 (2007).
[71] T. R. Slatyer, Phys. Rev. D **93**, 023521 (2016).
[72] L. Zhang, X.-L. Chen, Y.-A. Lei, and Z.-G. Si, Phys. Rev. D **74**, 103519 (2006).
[73] Y. Yang, Mon. Not. R. Astron. Soc. **486**, 4569 (2019).
[74] S. Clark, B. Dutta, Y. Gao, Y.-Z. Ma, and L. E. Strigari, Phys. Rev. D **98**, 043006 (2018).
[75] Y. Yang, Phys. Rev. D **91**, 083517 (2015).
[76] M. S. Madhavacheril, N. Sehgal, and T. R. Slatyer, Phys. Rev. D **89**, 103508 (2014).
[77] P. Stöcker, M. Krämer, J. Lesgourgues, and V. Poulin, J. Cosmol. Astropart. Phys. 03 (2018) 018.
[78] D. Blas, J. Lesgourgues, and T. Tram, J. Cosmol. Astropart. Phys. 07 (2011) 034.
[79] Y. Yang, Phys. Rev. D **102**, 083538 (2020).
[80] D. T. Cumberbatch, M. Lattanzi, J. Silk, M. Lattanzi, and J. Silk, Phys. Rev. D **82**, 103508 (2010).
[81] B. Ciardi and P. Madau, Astrophys. J. **596**, 1 (2003).
[82] Y. Yang, Phys. Rev. D **98**, 103503 (2018).
[83] Q. Yuan, B. Yue, X.-J. Bi, X. Chen, and X. Zhang, J. Cosmol. Astropart. Phys. 10 (2010) 023.
[84] M. Kuhlen, P. Madau, and R. Montgomery, Astrophys. J. **637**, L1 (2006).
[85] H. Liszt, Astron. Astrophys. **371**, 698 (2001).
[86] Y. Yang, Eur. Phys. J. Plus **131**, 432 (2016).
[87] S. R. Furlanetto, S. P. Oh, and E. Pierpaoli, Phys. Rev. D **74**, 103502 (2006).
[88] J. L. Bernal, A. Raccanelli, L. Verde, and J. Silk, J. Cosmol. Astropart. Phys. 05 (2018) 017; 01 (2020) E01.
[89] M. Kesden, A. Cooray, and M. Kamionkowski, Phys. Rev. Lett. **89**, 011304 (2002).
[90] D. Oberoi and J.-L. Pincon, arXiv:astro-ph/0312171.
[91] S. Jester and H. Falcke, New Astron. Rev. **53**, 1 (2009).
[92] S. Jester and H. Falcke, New Astron. Rev. **53**, 1 (2009).
[93] P. Platania, M. Bensadoun, M. Bersanelli, G. De Amici, A. Kogut, S. Levin, D. Maino, and G. F. Smoot, Astrophys. J. **505**, 473 (1998).
[94] C. G. T. Haslam, C. J. Salter, H. Stoffel, and W. E. Wilson, Astron. Astrophys. Suppl. Ser. **47**, 1 (1982).
[95] K. D. Lawson, C. J. Mayer, J. L. Osborne, and M. L. Parkinson, Mon. Not. R. Astron. Soc. **225**, 307 (1987).
[96] Planck Collaboration, Astron. Astrophys. **594**, A25 (2016).

[97] M. Valdes, A. Ferrara, M. Mapelli, and E. Ripamonti, Mon. Not. R. Astron. Soc. **377**, 245 (2007).
[98] J. O. Burns, Phil. Trans. R. Soc. A **379**, 20190564 (2021).
[99] A. Dolgov and J. Silk, Phys. Rev. D **47**, 4244 (1993).
[100] B. J. Carr, K. Kohri, Y. Sendouda, and J. Yokoyama, Phys. Rev. D **94**, 044029 (2016).
[101] S. Clesse and J. García-Bellido, Phys. Rev. D **92**, 023524 (2015).
[102] K. Kannike, L. Marzola, M. Raidal, and H. Veermäe, J. Cosmol. Astropart. Phys. 09 (2017) 020.
[103] J. Yokoyama, Phys. Rev. D **58**, 107502 (1998).
[104] J. C. Niemeyer and K. Jedamzik, Phys. Rev. D **59**, 124013 (1999).
[105] B. Carr, M. Raidal, T. Tenkanen, V. Vaskonen, and H. Veermäe, Phys. Rev. D **96**, 023514 (2017).
[106] A. M. Green, Phys. Rev. D **94**, 063530 (2016).
[107] N. Bellomo, J. L. Bernal, A. Raccanelli, and L. Verde, J. Cosmol. Astropart. Phys. 01 (2018) 004.
[108] B. Carr and F. Kuhnel, Annu. Rev. Nucl. Part. Sci. **70**, 355 (2020).
[109] F. Kühnel and K. Freese, Phys. Rev. D **95**, 083508 (2017).
[110] P. Villanueva-Domingo and K. Ichiki, Publ. Astron. Soc. Jpn. 119 (2022).
[111] H. Tashiro and N. Sugiyama, Mon. Not. R. Astron. Soc. **435**, 3001 (2013).
[112] P. S. Cole and J. Silk, Mon. Not. R. Astron. Soc. **501**, 2627 (2021).
[113] N. Afshordi, P. McDonald, and D. N. Spergel, Astrophys. J. Lett. **594**, L71 (2003).
[114] R. Hlozek *et al.*, Astrophys. J. **749**, 90 (2012).
[115] S. Bird, H. V. Peiris, M. Viel, and L. Verde, Mon. Not. R. Astron. Soc. **413**, 1717 (2011).
[116] J. L. Tinker, E. S. Sheldon, R. H. Wechsler, M. R. Becker, E. Rozo, Y. Zu, D. H. Weinberg, I. Zehavi, M. R. Blanton, M. T. Busha, and B. P. Koester, Astrophys. J. **745**, 16 (2012).
[117] C. Germani and T. Prokopec, Phys. Dark Universe **18**, 6 (2017).
[118] C. T. Byrnes, P. S. Cole, and S. P. Patil, J. Cosmol. Astropart. Phys. 06 (2019) 028.
[119] S. Passaglia, W. Hu, and H. Motohashi, Phys. Rev. D **99**, 043536 (2019).
[120] R. Zhai, H. Yu, and P. Wu, Phys. Rev. D **106**, 023517 (2022).
[121] R. N. Raveendran, K. Parattu, and L. Sriramkumar, Gen. Relativ. Gravit. **54**, 91 (2022).
[122] Y.-F. Cai, X.-H. Ma, M. Sasaki, D.-G. Wang, and Z. Zhou, arXiv:2207.11910.
[123] S. Heydari and K. Karami, J. Cosmol. Astropart. Phys. 03 (2022) 033.
[124] Z. Yi, Q. Gao, Y. Gong, and Z.-h. Zhu, Phys. Rev. D **103**, 063534 (2021).
[125] C. Ünal, E. D. Kovetz, and S. P. Patil, Phys. Rev. D **103**, 063519 (2021).
[126] R.-G. Cai, Z.-K. Guo, J. Liu, L. Liu, and X.-Y. Yang, J. Cosmol. Astropart. Phys. 06 (2020) 013.
[127] S. S. Mishra and V. Sahni, J. Cosmol. Astropart. Phys. 04 (2020) 007.
[128] A. Kalaja, N. Bellomo, N. Bartolo, D. Bertacca, S. Matarrese, I. Musco, A. Raccanelli, and L. Verde, J. Cosmol. Astropart. Phys. 10 (2019) 031.
[129] P. Carrilho, K. A. Malik, and D. J. Mulryne, Phys. Rev. D **100**, 103529 (2019).
[130] T.-J. Gao and Z.-K. Guo, Phys. Rev. D **98**, 063526 (2018).
[131] Z. Zhou, J. Jiang, Y.-F. Cai, M. Sasaki, and S. Pi, Phys. Rev. D **102**, 103527 (2020).
[132] Y.-F. Cai, X. Tong, D.-G. Wang, and S.-F. Yan, Phys. Rev. Lett. **121**, 081306 (2018).
[133] A. Ashoorioon, A. Rostami, and J. T. Firouzjaee, J. High Energy Phys. 07 (2021) 087.
[134] A. Ashoorioon, A. Rostami, and J. T. Firouzjaee, Phys. Rev. D **103**, 123512 (2021).